

Identification of anthropogenic and natural dust sources using Moderate Resolution Imaging Spectroradiometer (MODIS) Deep Blue level 2 data

Paul Ginoux,¹ Dmitri Garbuзов,² and N. Christina Hsu³

Received 1 May 2009; revised 21 October 2009; accepted 27 October 2009; published 9 March 2010.

[1] Mineral dust interacts with radiation and impacts both the regional and global climate. The relative contribution of natural and anthropogenic dust sources, however, remains largely uncertain. Although human activities disturb soils and therefore enhance wind erosion, their contribution to global dust emission has never been directly evaluated because of a lack of data. The retrieval of aerosol properties over land, including deserts, using the Moderate Resolution Imaging Spectroradiometer Deep Blue algorithm makes the first direct characterization of the origin of individual sources possible. In order to separate freshly emitted dust from other aerosol types and aged dust particles, the spectral dependence of the single scattering albedo and the Angstrom wavelength exponent are used. Four years of data from the eastern part of West Africa, which includes one of the most active natural dust sources and the highest population density on the continent, are processed. Sources are identified on the basis of the persistence of significant aerosol optical depth from freshly emitted dust, and the origin is characterized as natural or anthropogenic on the basis of a land use data set. Our results indicate that although anthropogenic dust is observed less frequently and with lower optical depth than dust from natural sources in this particular region, it occupies a large area covering most of northern Nigeria and southern Chad, around Lake Chad. In addition, smaller anthropogenic sources are found as far south as 5° of latitude north, well outside the domain of most dust source inventories.

Citation: Ginoux, P., D. Garbuзов, and N. C. Hsu (2010), Identification of anthropogenic and natural dust sources using Moderate Resolution Imaging Spectroradiometer (MODIS) Deep Blue level 2 data, *J. Geophys. Res.*, 115, D05204, doi:10.1029/2009JD012398.

1. Introduction

[2] Mineral dust affects the climate by absorbing and scattering solar and terrestrial radiation as well as by modifying cloud properties [Forster *et al.*, 2007]. Its long range transport and deposition over open oceans also provides a nutrient for phytoplankton blooming [Martin *et al.*, 1991], which modulates carbon sequestration. It has also been suggested that African dust is an essential nutrient for the Amazon forest [Swap *et al.*, 1992], which is a major sink of CO₂. The evaluation of these effects with climate models contains many uncertainties including characterizing sources as natural or anthropogenic, which is vital as only the anthropogenic component contributes to radiative forcing on the climate [Forster *et al.*, 2007]. Human activities that contribute to anthropogenic sources include herding livestock, agriculture, mining, construction, off-road vehicles, and war [Zender *et al.*, 2004].

[3] Most studies infer indirectly anthropogenic contribution to dust loading by suggesting that it provides the best explanation for an observed increase of dust loading or deposition or to reconcile discrepancy between models and observations. Moulin and Chiapello [2006] have suggested that the observed increase of a factor of 2 of background dust loads over the Atlantic since the mid-1960s can be attributed to human-induced soil degradation in Sahel, independent of any climatic phenomenon. Neff *et al.* [2008] have linked an increase of dust deposition in the western United States to expansion of livestock grazing in the early twentieth century. In West Africa, comparing simulated and observed aerosol indices (AIs) in the near-ultraviolet, Yoshioka *et al.* [2005] found that the best comparison at the Sahara-Sahel border is obtained by adding 20%–25% of dust from disturbed soils. Similar magnitude was inferred by Mahowald *et al.* [2007] using visibility data from meteorological stations. Another difficulty to attribute dust from anthropogenic sources is that dust emission from roads, factories, or construction sites may be fugitive and of relatively small scale. On the other hand, natural sources are relatively well characterized and have been inferred to be located preferentially in topographic depression with bare and dry soils by Prospero *et al.* [2002] using satellite data. The use of preferential locations for

¹Geophysical Fluid Dynamics Laboratory, NOAA, Princeton, New Jersey, USA.

²Department of Computer Sciences, Princeton University, Princeton, New Jersey, USA.

³NASA Goddard Space Flight Center, Greenbelt, Maryland, USA.

modeling dust has yielded satisfactory simulations of dust distribution when compared with observations [Ginoux *et al.*, 2001; Tegen *et al.*, 2002; Zender *et al.*, 2003]. However, Mahowald and Luo [2003] have shown that due to the distance between dust sources and observation as well as model uncertainties an anthropogenic contribution approaching 50% is within the range of uncertainty.

[4] Satellite instruments provide near-daily global data with retrieved information on aerosol properties which have been used to locate natural sources over arid and semiarid regions. Different methods have been proposed on the basis of the characteristics of the sensor bands (e.g., Legrand *et al.* [2001] or Schepanski *et al.* [2007] in the infrared or Prospero *et al.* [2002] in the near-ultraviolet). However, these methods were not applied in temperate or tropical areas with more obvious human activity because of the complexity of aerosol composition in those areas. In arid regions, extinction can be attributed primarily to mineral dust, but elsewhere sulfate, sea-salt, or carbonaceous aerosols, which are not emitted from soils, absorb and scatter light more efficiently. Detecting dust among other aerosols, however, relies on the retrieval of spectral optical properties. Another drawback of using a single wavelength aerosol property is the difficulty to distinguish freshly emitted dust from aged dust. This may be particularly true for slow moving dust plumes observed [Bou Karam *et al.*, 2008]. Unfortunately, no satellite algorithm provided near-global daily distribution of aerosol properties at multiple wavelengths at a spatial resolution sufficient to detect small scale anthropogenic dust sources until recently.

[5] Hsu *et al.* [2004] have developed an algorithm using multiple radiances, including the 412 nm channel, measured by the Moderate Resolution Imaging Spectroradiometer (MODIS). Their products include near-global daily optical depth (τ), single scattering albedo (ω), and Angstrom wavelength exponent (α) at about 10 km resolution. These products are provided operationally at about 10 km and 1° resolution for level 2 and 3 data sets, respectively. Knowing the typical spectral variation of dust optical properties, it is finally possible with these satellite products to identify dust sources. However, anthropogenic activities do not change the optical properties of dust, and additional information is needed to distinguish between anthropogenic and natural sources.

[6] In this paper, we combine land use data set and direct satellite measurements to identify natural and anthropogenic dust sources. We select a domain to include a very intense natural source and a country with high population density. In sections 3 and 4, we briefly describe the gridded level 2 MODIS Deep Blue (MODIS DB) products and the domain selection before presenting our methodology to locate natural and anthropogenic dust sources and comparing with other studies. Then we attempt to quantify the importance of anthropogenic sources relative to natural sources, followed by a short evaluation of our method using plots on GoogleEarth™. Finally, we present our conclusions.

2. Level 2 MODIS DB Data

[7] The Deep Blue algorithm employs radiances from the blue channels of satellite instruments, at which wavelengths the surface reflectance is low enough that the presence of

dust brightens the total reflectance and enhances the spectral contrast [Hsu *et al.*, 2004]. The Deep Blue algorithm has been applied operationally since April 2007 to the MODIS instrument on the Aqua platform. A detailed description of the algorithm is given by Hsu *et al.* [2004], and we present only a brief overview. After screening for clouds, the surface reflectance for a given pixel is determined from a clear-scene database on the basis of its geolocation. The reflectance at 412, 470, and 670 nm is compared with pre-calculated radiances at different viewing angles, surface reflectance, τ , and ω [Hsu *et al.*, 2006]. Then, a minimization procedure is applied to determine the mixing ratio of various dust to smoke models that best fits the calculated and observed spectral reflectance. For the particular mixing ratio that produces the best match, the values of τ and ω at 412, 550, and 670 nm, and α are reported. The pixel values are then averaged over 10 km cells and aggregate into granules of approximately 1500×2000 cells, forming MODIS-Aqua collection 5.0 level 2 data. These data are available daily over bright surface (reflectance at 550 nm greater than 0.15) and from August 2002 (with further backward processing still continuing) to present. The 1° resolution gridded version constitutes MODIS-Aqua collection 5.0 level 3. Since November 2008, the algorithm includes updated characterization of surface bidirectional reflectance distribution function (BRDF) and cloud screening techniques. Although the reprocessed data are available in collection 5.1, which provides better quality assurance for the retrieved products, our study uses collection 5.0. As our method does not depend on absolute values, the improvements introduced in collection 5.1 should not affect our results. Our scheme for the detection of dust sources is facilitated by working with data on a regular latitude and longitude grid (level 3 data) rather than on irregularly spaced pixels along the orbit track (level 2 data). A drawback of the existing level 3 data is that the 1° resolution is too coarse to accurately detect small scale anthropogenic sources. Therefore, we have interpolated the level 2 data on a regular latitude \times longitude grid with a 0.1° spacing. First, all pixels covering part of the domain are concatenated into one daily file. Then, a linear interpolation is performed at every fixed grid point by weighting the level 2 values surrounding a fixed grid point by the fraction of overlapping area between the two grids. This method conserves the spatially integrated data. The algorithm is repeated for every day from 1 January 2003 to 31 December 2006.

3. Domain Selection

[8] The domain is chosen to cover one of the most active and well studied natural source, the Bodélé depression in Chad [Prospero *et al.*, 2002; Washington *et al.*, 2006; Todd *et al.*, 2007], and the country with the highest population density (~ 140 hab.km $^{-2}$) in Africa, Nigeria, where intensive overgrazing by large cattle herds has been well documented in the northern part of the country [Mortimore and Adams, 1999]. The domain extends from 0° to 20° longitude east and 5° to 20° latitude north and corresponds to the eastern part of West Africa. In West Africa, the activity of dust sources depends on their position relative to the Intertropical Convergence Zone (ITCZ), which occupies its southernmost position (about 5°N) in December and

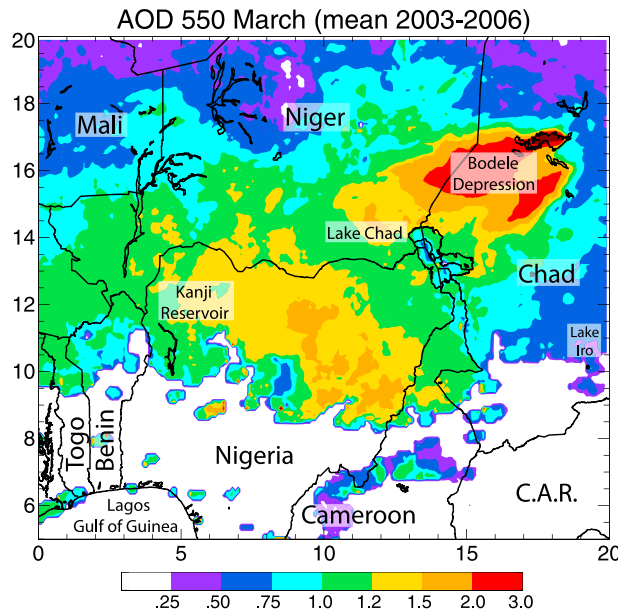


Figure 1. Monthly mean MODIS Deep Blue aerosol optical depth at 550 nm for March averaged from 2003 to 2006 on a fixed grid with 0.1° resolution. Country names and geographic features are indicated in black and dark gray, respectively.

northern most position (about 15°N) in July [Ginoux et al., 2001]. During the dry season in the Sahel (arid region of West Africa south of 20°N), from December to February, dust sources are very active while at the same time large amount of carbonaceous aerosols are emitted by biomass burning. In summer, the area south of the ITCZ receives abundant precipitation, which shuts down biomass burning and dust emission. During this season, there is no aerosol retrieval from MODIS data due to clouds. Therefore, the best period to detect dust sources is in early spring, as the biomass burning activities weaken and before the moist air from the Gulf of Guinea has penetrated north of 6°N [Hastenrath, 1991]. Figure 1 shows the yearly distribution of monthly mean τ (550 nm) distribution for March, from year 2003 to 2006. The highest values of τ at 550 nm, between 2 and 3, are observed along two plumes originating from ephemeral lakes in the Bodélé depression (black contours on the northwest side of the red shading). The southwest orientation is typical of the trade winds in West Africa, called the Harmattan. Another large maximum, with values greater than 1, occupies the northern part of Nigeria. There are also many localized maxima from the Gulf of Guinea to 10° latitude north.

4. Dust Source Detection

[9] Prospero et al. [2002] have shown that persistent dust sources can be identified from the frequency-of-occurrence (FOO) of the Total Ozone Mapping Spectrometer (TOMS) absorbing aerosol index, used as a proxy for atmospheric dust. A limitation of their approach is the dependency of the absorbing aerosol index on all UV absorbing aerosols, which include not only dust but also carbonaceous aerosol. Aware of this dependency, they limit their study to arid and

semiarid regions where there are no significant biomass burning activities. Here, we also use FOO to localize dust sources, but by taking advantage of the spectral aerosol properties retrieved from MODIS Deep Blue we extend our study beyond arid regions. FOO is calculated as the number of days τ (550 nm) is greater than a threshold value (τ_{thresh}), and α and ω satisfy criteria of freshly emitted dust particles. Freshly emitted dust is characterized by large particles which have not yet been removed by gravitational settling. Maring et al. [2003] have observed that particles greater than 7.3 μm are efficiently removed during transport, but once the largest particles are removed the normalized size distribution does not change over days. The rapid shift of size distribution from coarse freshly emitted dust toward stable fine aged dust provides a powerful method to isolate sources from lingering dust. Also, there is a strong contrast between coarse mode dust particles and accumulation mode (particle radius less than 0.5 μm) of biomass burning and urban aerosols. Therefore, a parameter sensitive to the size distribution should allow the separation of not only dust from other aerosol types, but also freshly emitted dust from aged dust. Eck et al. [1999] have shown that the dominance of one mode over the other on τ can be measured with the Angstrom wavelength exponent α . The α values range from -0.5 to 1 in dusty environment and higher in polluted regions [Dubovik et al., 2002]. As the largest particles are removed from the atmosphere by gravitational settling, aged dust will contain smaller particles characterized by a higher α value. In case of other coarse particles, such as sea salt aerosol, we use only cases of increasing ω with wavelength, or $\omega_{670} - \omega_{412} > 0$. This is similar to imposing increasing absorption from red to blue wavelengths, which is a typical optical property of dust but not for sea salt which does not absorb in the visible [Dubovik et al., 2002]. Figure 2 shows the distribution of τ , α and $\omega_{670} - \omega_{412}$ for 3 March 2005. In the upper part, τ distribution has two distinct maxima, one over Bodélé depression and one in northern Nigeria. The plumes in the Bodélé depression originate from ephemeral lakes, as was observed on many occasions [e.g., Prospero et al., 2002; Koren and Kaufman, 2004]. There are also some dispersed localized maxima extending to the Gulf of Guinea. The α values are roughly negative in the northern part corresponding to deserts and greater than 1 in the southern part associated with savannah and forests. Some spots in the southern region have negative values, indicating the presence of dust. The ω spectral contrast is essentially positive except in northern Nigeria where there are negative values, typical of black carbon aerosols. It appears that α offers a more stringent constraint on the data than $\omega_{670} - \omega_{412}$. However, we keep both criteria to detect dust.

[10] Figure 3 illustrates the sensitivity of filtering α to the calculation of FOO with $\tau > \tau_{\text{thresh}}$ for two different values of τ_{thresh} (0.25 and 1). It should be noted that FOO is calculated for the total number of days with $\tau > 0$, in order to compare equal area with missing data, because of the presence of clouds or dark surface (surface reflectivity < 0.15). In this figure, the statistics are built for each year, and the mean FOO over 4 years is plotted. Without constraint on α , τ is greater than 0.25 for more than 80% of the time, but for $\tau > 1$ a similar percentage is only observed over the central ephemeral lake in the Bodélé depression. In other

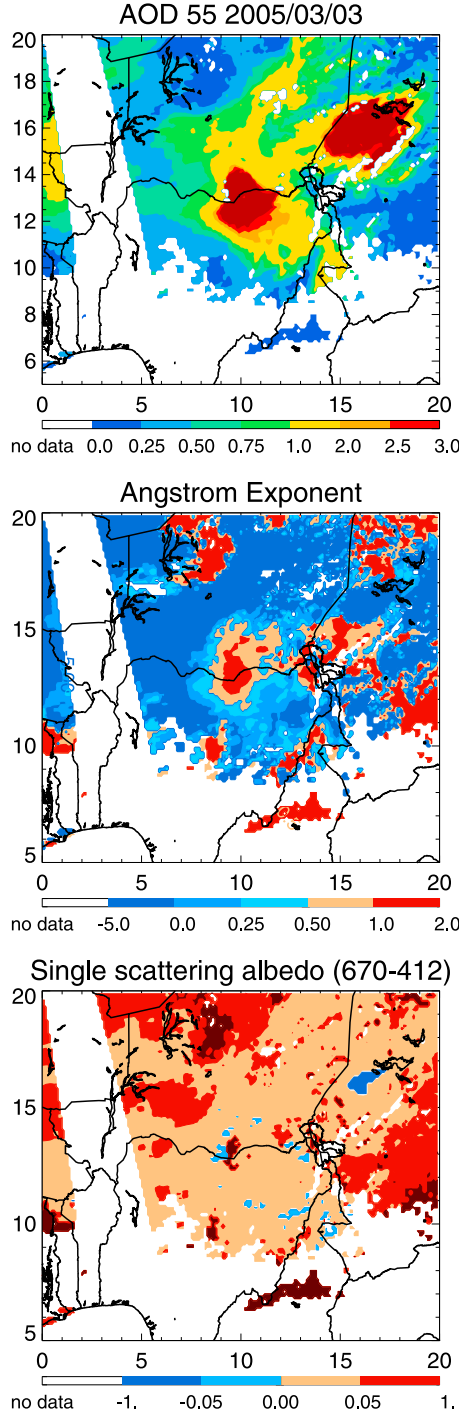


Figure 2. (Upper) Daily aerosol optical depth at 550 nm, (middle) Angstrom exponent, and (lower) difference of single scattering albedo between 670 and 412 nm on 3 March 2005.

words, after increasing τ_{thresh} , FOO maxima are found mainly over source locations and weaker sources are screened out. Constraining α allows us to use a relatively low value of τ_{thresh} , as can be seen in Figure 2. Indeed with $\alpha_{\text{thresh}} = 0.5$ or 0 and low τ_{thresh} , hot spots appear more clearly and are located primarily in Niger and Chad but are also present in northern Nigeria with maxima around Lake Chad. Figure 4 shows the seasonal variation of the FOO

averaged over 4 years (2003–2006) for $\tau_{\text{thresh}} = 1$ and $\alpha_{\text{thresh}} = 0$. For all seasons, the highest frequencies are within the ephemeral lakes of the Bodélé depression. Outside these lakes but within the Bodélé depression there is all yearlong dust activity. Such yearly activity is also noticeable on the northern shore of Lake Chad. Spring is the season with the largest spread of source activity reaching farthest south in Nigeria and Cameroon. The lowest activity appears in fall. These seasonal properties do not change significantly from year to year or for lower value of τ_{thresh} (not shown), so the best period to detect dust sources from human activities is in spring, which shows the highest FOO in northern Nigeria and Lake Chad region.

5. Comparison With Other Studies

[11] The first aerosol product retrieved globally was the aerosol index derived by *Herman et al.* [1997] using the TOMS measurements in the near ultraviolet. *Prospero et al.* [2002] have shown that the most frequent location of the maxima of TOMS AI in arid or semiarid regions is over topographic depression and can be associated with the presence of ephemeral lakes. Because of the coupling molecular-aerosol scattering in the ultraviolet, TOMS AI depends almost linearly on the altitude of the plume [*Ginoux and Torres*, 2003]. As the sensitivity near the surface is reduced, the source location is biased toward downwind area as it has been shown by *Mahowald et al.* [2007]. Although the exact location of dust sources from TOMS may be slightly biased, a study by *Engelstaedter et al.* [2003] using visibility data confirmed that dust storm frequency increases with the fraction of topographic depression. As MODIS DB algorithm is using wavelength in the visible, although near the ultraviolet part of the visible spectrum, the retrieval is much less sensitive to the altitude of the aerosol layer [*Hsu et al.*, 2006]. A second uncertainty in our results may be related to the time of sampling by MODIS instrument. Polar orbiting satellite instruments, like TOMS or MODIS, have a local passing time which may not necessarily correspond to the peak of dust emission. *Ginoux and Torres* [2003] presented a detailed analysis of TOMS AI dependencies and showed that TOMS passing time at 11:30 am does not always correspond to the maximum frequency of diurnal variation of friction velocity. Comparing the distribution of source activity over West Africa, derived from TOMS AI and from geostationary infrared data, *Schepanski et al.* [2007] explain the difference between the two by the fact that the time of dust activity is ahead of TOMS passing time. In our case, we use MODIS on Aqua platform which has a local passing time at 1:30 pm. This is even later than TOMS. But as long as a source is statistically active throughout the day, it can be detected by MODIS as was shown by *Koren and Kaufman* [2004] in the case of the Bodélé depression. *Schepanski et al.* [2009] provided from satellite infrared data the diurnal variation of the frequency of dust storms for nine regions in West Africa. In all regions, the frequency of dust storms is never null between noon and 3 pm. We are using 4 years of daily data and this should provide satisfactory representation of source activity even for sources with maximum activity earlier than MODIS passing time. *Koren and Kaufman* [2004] using 500 m resolution MODIS data showed that

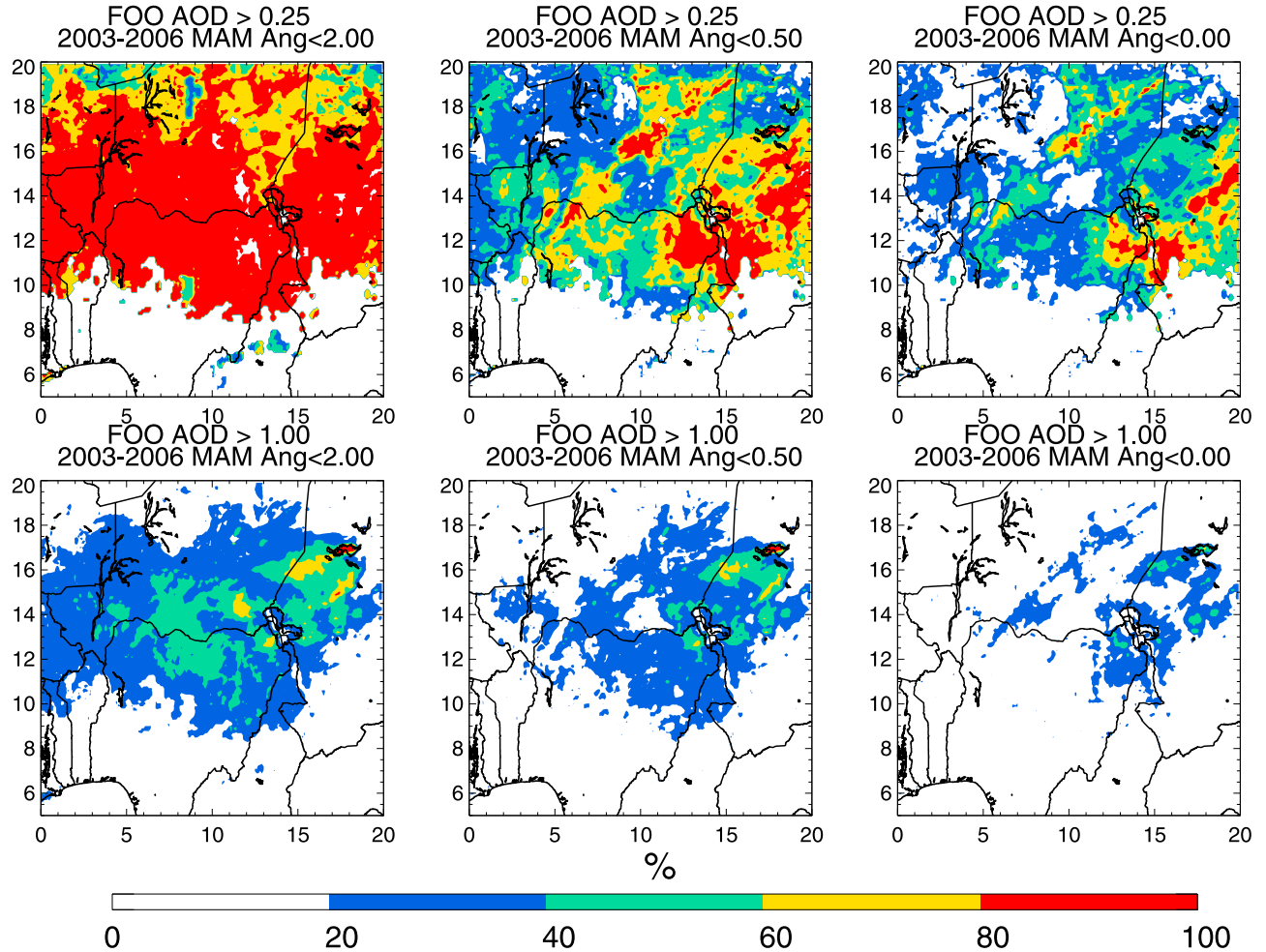


Figure 3. (Upper) Variability of FOO distribution with $\tau_{\text{thresh}} = 0.25$ and (lower) and $\tau_{\text{thresh}} = 1$ when the data are constrained with Angstrom exponent less than (left) 2, (middle) 0.5, and (right) 0. The units are percentage of days satisfying the criteria by the total number of days with nonmissing MODIS data per year, and averaged from 2003 to 2006.

dust source in the Bodélé depression correspond with the ephemeral lakes characterized by large deposits of white diatoms. Figure 4 shows that our technique with slightly coarser resolution agree with their study. *Schepanski et al.* [2007] presented seasonal variation of dust activity on a 1° resolution grid. Figure 4 shows similarities with their results. First, the Bodélé depression is active all yearlong. Second, there is all yearlong dust activity in Niger, which is not obvious by *Prospero et al.* [2002] results. Third, spring is the season with the southernmost dust activity. Fourth, there is all yearlong dust activity along the northern shore of Lake Chad. On the other hand, the most active season along the Sahara-Sahel border appears in winter in their analysis, while in our case it is in spring. A more quantitative comparison would be useful to evaluate and understand such discrepancy.

6. Natural and Anthropogenic Sources

[12] Human activities may affect wind erosion directly by disturbing soil properties or indirectly through the increased desertification associated with climate change. In this anal-

ysis, we attempt to locate instances of the former. There is currently no data set that provides the geographic distribution of disturbed soils, but inventories of land use are available at a resolution comparable with our data. To attribute an anthropogenic or natural origin to a dust source, we assume that any source within a grid cell with 10% or more land use (croplands and pastures) is anthropogenic; otherwise it is natural. The fraction of grid cells containing changes in land cover by croplands and pastures for the year 2000 is obtained from the 8 km resolution HYDE database [*Klein Goldewijk*, 2001]. Figure 5 shows the distribution of FOO where τ is greater than 0.25, 0.5, 0.75, and 1 at 550 nm over a year and the average over 4 years (2003–2006). Figure 5 also shows the distribution of land use exceeding 10% and the estimated anthropogenic and natural contribution to dust. Most of the domain south of 16°N shows significant land use with values up to 85% in northern Nigeria and southern Chad, around Lake Chad. In Benin, Cameroon, and Central African Republic, there are large untouched areas. The maxima of FOO distribution for different values of τ_{thresh} show a similar pattern up to 0.75. Beyond this value, they appear essentially between

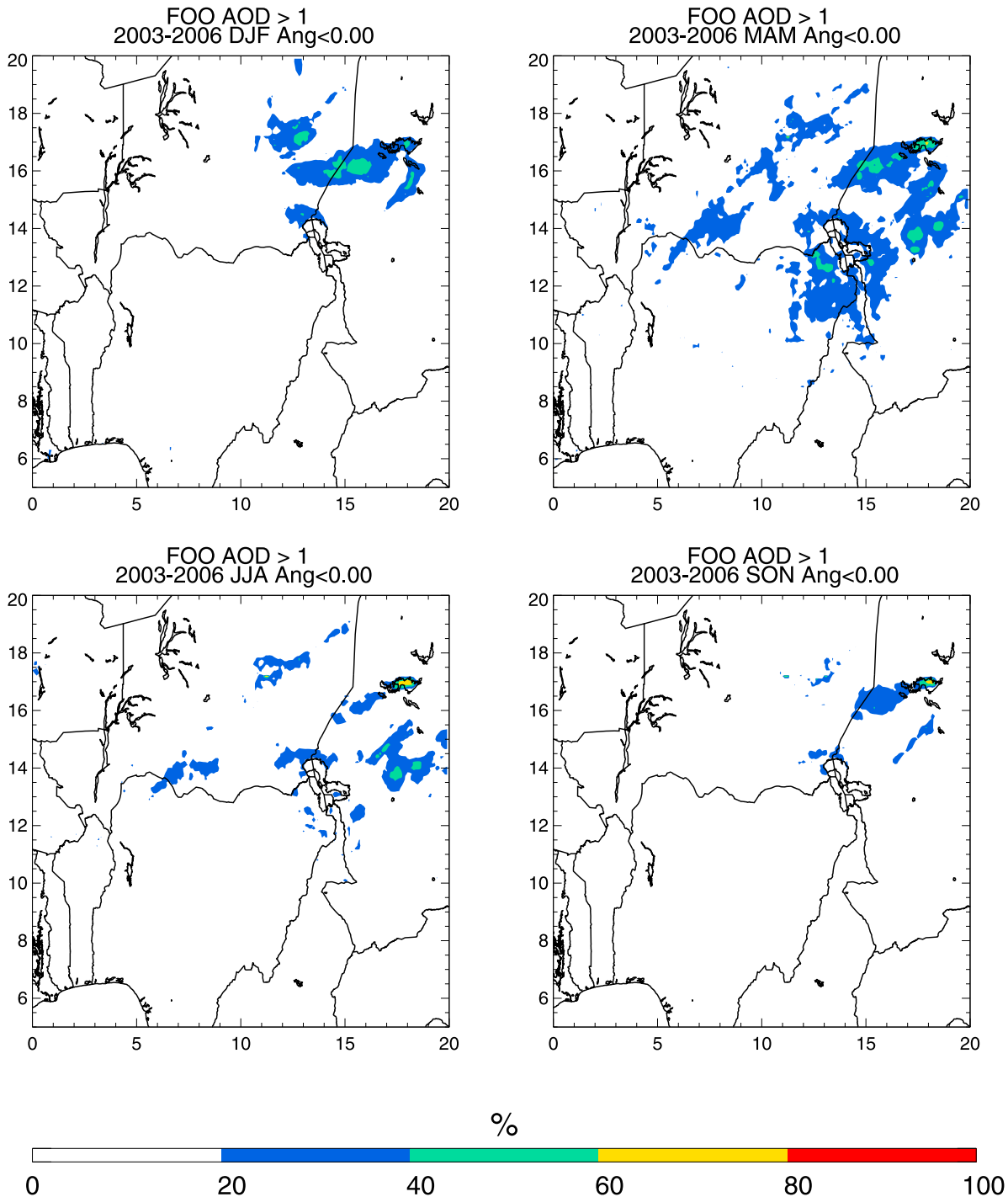


Figure 4. Seasonal variation of FOO distribution with $\tau_{\text{thresh}} = 1$ and $\alpha_{\text{thresh}} = 0$: (upper left) December–January–February, (upper right) March–April–May, (lower left) June–July–August, (lower right) and September–October–November. The units of FOO are percentage of days satisfying the criteria by the total number of days with nonmissing MODIS data per year, and averaged from 2003 to 2006.

Lake Chad and Bodélé with some hot spots along the Gulf of Guinea. In terms of the origins of these sources, there seems to be a symmetric distribution of FOO >20% on both sides of the 16° parallel. However, the frequencies are twice as high or more north of this parallel, where land use indicates that the sources are natural in origin. Also, there appear to be several natural sources in Benin and Cameroon

with τ greater than 0.5 for at least 20% of the time. To evaluate the relative importance of anthropogenic sources, we calculate in Table 1 the surface area occupied by the different isocontours of Figure 5. The total surface area of the domain is 3.6 million km². Over roughly 50%, 25%, 10%, and 2.5% of the domain and for more than 20% of the time with valid data, τ is greater than 0.25, 0.5, 0.75, and

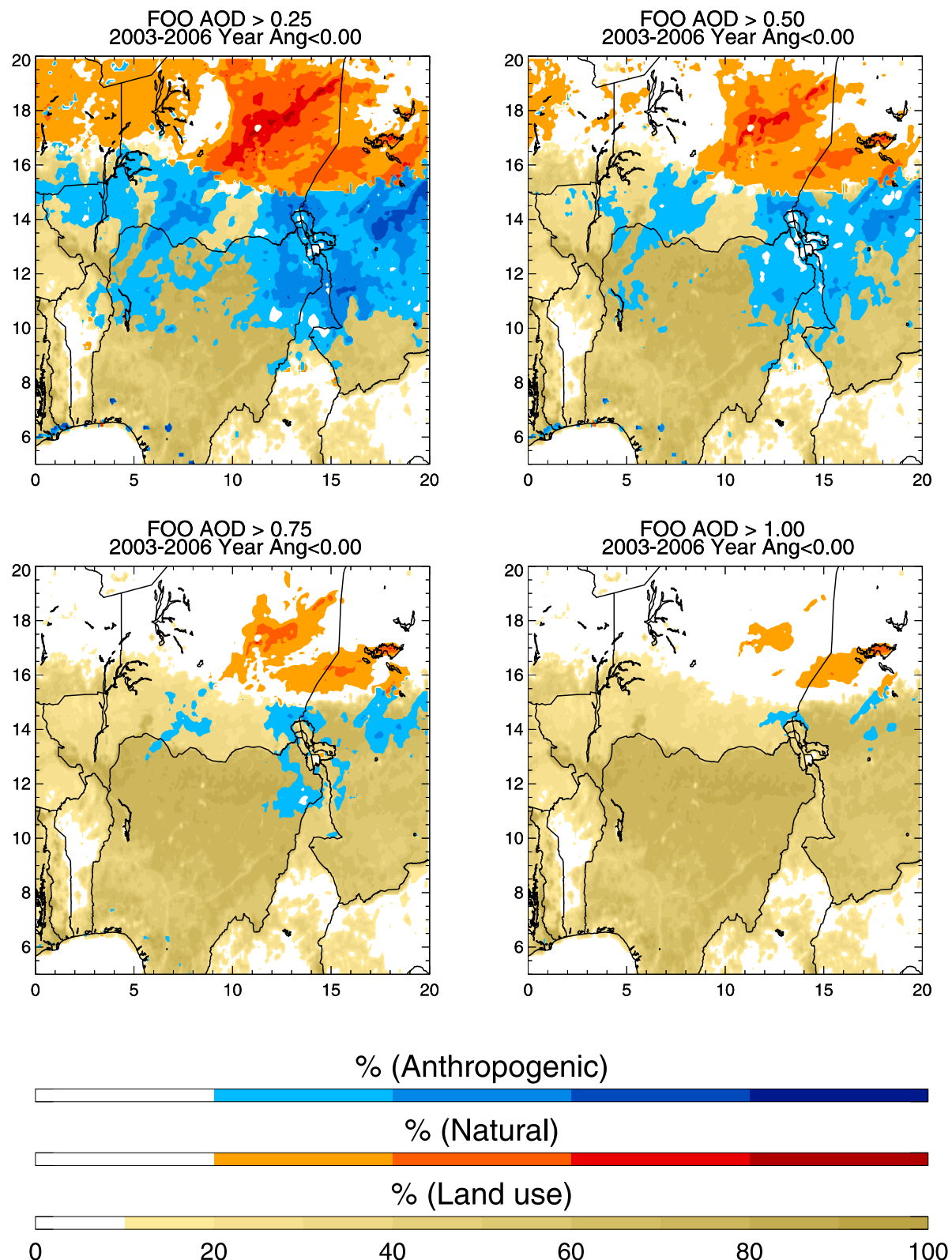


Figure 5. Distribution of natural (red shading) and anthropogenic (blue shading) FOO with $\alpha_{\text{thresh}} = 0$ and (upper left) $\tau_{\text{thresh}} = 0.25$, (upper right) 0.5, (lower left) 0.75, and (lower right) 1, overplotted on the percentage land use (croplands and pastures) from 10% to 100% (in yellow, the lighter the color the higher the percentage of land use). The units of FOO are percentage of days satisfying the criteria by the total number of days with nonmissing MODIS data per year, and averaged from 2003 to 2006.

Table 1. Surface Area of Natural and Anthropogenic Sources of τ (550 nm) Greater than 0.25, 0.5, 0.75, and 1 for Frequency of Occurrence Greater than 20%, 40%, 60%, and 80%^a

τ	FOO > 20%			FOO > 40%			FOO > 60%			FOO > 80%		
	N (10^6 km^2)	A (10^6 km^2)	A/(A + N) (%)	N (10^6 km^2)	A (10^6 km^2)	A/(A + N) (%)	N (10^6 km^2)	A (10^6 km^2)	A/(A + N) (%)	N (10^6 km^2)	A (10^6 km^2)	A/(A + N) (%)
0.25	786	942	54	302	290	49	57	37	40	6	1.5	19
0.5	472	530	53	109	64	37	13	2.8	18	0.3	0.2	41
0.75	193	167	46	27	4.9	15	0.9	0	0	0	0	0
1	75	25	25	4.5	0	0	0.2	0	0	0	0	0

^aThe percentage of anthropogenic surface relative to total dusty surface (A/(A + N)), where N is natural and A is anthropogenic, is also given for each case.

1.0, respectively. Out of these regions, 50% is occupied by anthropogenic dust for a value of optical depth less than 0.75. This percentage decreases as the frequency of occurrence increases, except for $\tau_{\text{thresh}} = 0.5$ where there is an equivalent surface at 80% FOO. For an optical depth of 0.75 or higher, only natural dust has a frequency of occurrence higher than 60%. As the choice of a minimum 10% land use was quite arbitrary, we calculate in Table 2 the percentage of anthropogenic source for 5%, 25%, and 50% minimum land use. For optical depth below 0.75, anthropogenic dust area appears relatively independent of the percentage of land use. But for higher optical depth, the surface area of anthropogenic dust decreases rapidly with an increasing cutoff value of land use. This is because a large fraction of dust with optical depth higher than 0.5 is located in southern Niger where the land use is between 20% and 50%. At lower optical depth a large fraction of dust is over northern Nigeria and southern Chad with land use much larger than 50%. These results indicate that anthropogenic sources may emit at low optical depth as much as 50% of all dust in that region and at least 20% of the time, while only natural sources can generate optical depth greater than 1 for more than 40% of the time. Although the anthropogenic sources appear weaker than natural sources, it is important to note that they are located further south than any previously studied dust sources in West Africa. This may increase the amount of long range transport of dust, mostly in winter, to the Amazon basin where it provides nutrients [Swap et al., 1992] and may also contribute to low elevation dust as observed during field experiment over Sahel [Osborne et al., 2008].

7. Evaluation

[13] The validation of our results with data is not possible as there are no ground observations of anthropogenic dust in this part of the world. One empirical method is to attempt to correlate the FOO maxima with either urban areas or known

natural features such as ephemeral lakes. Using high resolution imagery of the Earth, such as GoogleEarth™, it is generally possible to determine the plausibility of an anthropogenic source detected using our methodology. We present several such cases where the characterization of dust sources in Nigeria and Chad is inaccurate or ambiguous. Figure 6 shows the 40% and 60% contours of FOO over Lake Iro in Chad, which is attributed to human activity on the basis of the existence of land use over the area. But its location on an ephemeral lake bed is not taken into account by our algorithm. Most likely, dust emission is generated from the dry lake bed in period of drought, in which case we should identify the source as natural. It is also possible that the river flow to the lake is diverted for irrigation, in which case the source should be identified as anthropogenic. This illustrates the limitation of using only the land use data set to classify dust sources. Figure 7 demonstrates a similar case where there is an equal attribution to anthropogenic and natural dust over the Kainji reservoir in Nigeria. Dust emission from dry lake beds is very effective and appears as an obvious natural source, but if the lake bed is exposed as a consequence of irrigation or over-pumping, the source should be considered solely as anthropogenic. Figure 8 shows a wrong attribution of natural dust over Lagos, capital of Nigeria due to the absence of pasture or cropland in mega cities. On the other hand, we found that most sources in Benin and Cameroon are wrongly attributed to natural



Figure 6. GoogleEarth image of Lake Iro ($10^{\circ}5'53.50''\text{N}$, $19^{\circ}24'59.20''\text{E}$) in Chad, with 40% and 60% FOO anthropogenic (blue semitransparent polygons) dust with $\tau_{\text{thresh}} = 0.25$ and $\alpha_{\text{thresh}} = 0$.

Table 2. Percentage of Anthropogenic Surface Relative to Total Dusty Surface for Three Values of Land Use Change, 5%, 25%, and 50%, and Four Minimum Values of FOO, 20%, 40%, 60%, and 80%

τ	FOO > 20%			FOO > 40%			FOO > 60%			FOO > 80%		
	5%	25%	50%	5%	25%	50%	5%	25%	50%	5%	25%	50%
0.25	57	48	33	50	45	34	40	38	32	21	16	10
0.5	55	48	34	38	33	26	20	16	11	41	41	41
0.75	47	41	29	16	13	8	0	0	0	0	0	0
1	26	18	11	0	0	0	0	0	0	0	0	0

origin as they appear, by zooming with GoogleEarth but not shown, centered on recently cleared land in forests. This error may be due to the fact that these clearings are more recent than the land use database. The surface areas of these wrong attributions are a few hundreds kilometer square and are insignificant compared with the total dust sources. However, in other regions, it may be necessary to obtain detailed information for each source individually. In that regard, high resolution data sets are crucial, and the overlaying of the FOO isocontours on GoogleEarth is of great help but not sufficient.

8. Summary and Conclusions

[14] In order to evaluate the anthropogenic contribution to dust emission from direct measurement, we have used the MODIS Deep Blue level 2 aerosol products in combination with land use data set. The daily MODIS products have been interpolated on a regular grid of 0.1° resolution from January 2003 to December 2006. Using the spectral values of single scattering albedo (ω) and the Angstrom wavelength exponent (α), the daily gridded data are screened for coarse dust particles by imposing the constraints $\alpha < 0$ and $\omega_{412} < \omega_{670}$. The frequency of occurrence of areas where the aerosol optical depth (τ) is greater than a threshold optical depth (τ_{thresh}) is calculated, and its seasonal and yearly distributions are used to locate dust sources. We select a domain which includes the most active natural dust source, the Bodélé, and Nigeria with the highest population density in Africa. The most permanent sources have higher FOO values and the most intense have higher τ_{thresh} for similar FOO.

[15] For low τ_{thresh} , yearly FOO is relatively uniformly distributed in the upper half of the domain but as we increase τ_{thresh} up to 1 only regions around Lake Chad and Bodélé appear active. The distribution of FOO shows a seasonal cycle with maxima in winter and fall over Niger, in spring over Chad and Nigeria, and in summer over Mali, Niger, and Chad. During all seasons there are hot spots over



Figure 8. GoogleEarth image of Lagos ($6^{\circ}32'0.12''\text{N}$, $3^{\circ}22'32.27''\text{E}$) in Nigeria, with 40% and 60% FOO natural (red semitransparent polygons) and anthropogenic (blue semitransparent polygon) dust with $\tau_{\text{thresh}} = 0.25$ and $\alpha_{\text{thresh}} = 0$.

Bodélé and around Lake Chad. Except in summer, when the ITCZ occupies its northernmost position and there are no data because of clouds, there are multiple local maxima around the Gulf of Guinea.

[16] The identification of anthropogenic or natural sources is performed by using land use data set. In regions where at least 5%–25% of the land surface is cultivated or otherwise disturbed, more than half of the domain is potentially an anthropogenic dust source. By overlaying the distribution of FOO, it appears that for $\tau < 0.75$, 50% of dust is anthropogenic but beyond such optical depth dust is essentially of natural origin. The anthropogenic sources are essentially located in northern Nigeria and western Chad around Lake Chad. Some local natural and anthropogenic sources are found as far south as the Gulf of Guinea.

[17] Evaluation of the results using GoogleEarth™ indicates some false or ambiguous identification. We show cases of a lake and reservoir where the attribution is ambiguous as it is not possible to determine whether the source arises because of climate drought or human activities without further information. These cases account for relatively small areas and should not modify our results significantly. But quantitative comparison with other data sets should provide more solid evaluation. This will be performed at the global scale in a follow-up paper.

[18] **Acknowledgments.** We are thankful to the reviewers comments who help us improve the manuscript. Dmitri Garbuзов was funded under the summer internship program by the Princeton Environmental Institute. Figures 6, 7, and 8 have been realized using GoogleEarth™.

References

- Bou Karam, D., C. Flamant, P. Knippertz, O. Reitebuch, J. Pelon, M. Chong, and A. Dabas (2008), Dust emissions over the Sahel associated with the West African monsoon intertropical discontinuity region: A representative case-study, *Q. J. R. Meteorol. Soc.*, *134*, 621–634, doi:10.1002/qj.244.
- Dubovik, O., B. Holben, T. F. Eck, A. Smirnov, Y. J. Kaufman, M. D. King, D. Tanre, and I. Slutsker (2002), Variability of absorption and optical properties of key aerosol types observed in worldwide locations, *J. Atmos. Sci.*, *59*, 590–608.

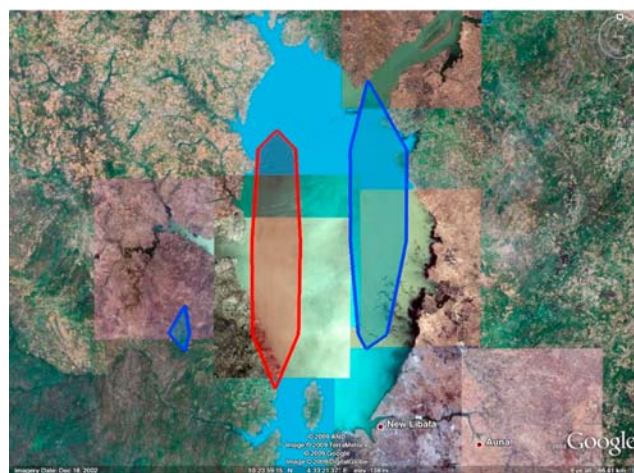


Figure 7. GoogleEarth image of Kainji reservoir ($10^{\circ}24'35.28''\text{N}$, $4^{\circ}32'45.90''\text{E}$) in Nigeria, with 40% FOO natural (red semitransparent polygon) and anthropogenic (blue semitransparent polygon) dust with $\tau_{\text{thresh}} = 0.25$ and $\alpha_{\text{thresh}} = 0$.

- Eck, T. F., B. N. Holben, J. S. Reid, O. Dubovik, A. Smirnov, N. T. O'Neill, I. Slutsker, and S. Kinne (1999), Wavelength dependence of the optical depth of biomass burning, urban, and desert dust aerosols, *J. Geophys. Res.*, 104(D24), 31,333–31,349.
- Engelstaedter, S., K. E. Kohfeld, I. Tegen, and S. P. Harrison (2003), Controls of dust emissions by vegetation and topographic depressions: An evaluation using dust storm frequency data, *Geophys. Res. Lett.*, 30(6), 1294, doi:10.1029/2002GL016471.
- Forster, P., et al. (2007), Changes in atmospheric constituents and in radiative forcing, in *Climate Change 2007: The Physical Science Basis, in Contribution of Working Group I to the Fourth Assessment Report of the Intergovernmental Panel on Climate Change*, edited by S. Solomon et al., pp. 129–234, Cambridge Univ. Press, Cambridge, U. K.
- Ginoux, P., and O. Torres (2003), Empirical TOMS index for dust aerosol: Applications to model validation and source characterization, *J. Geophys. Res.*, 108(D17), 4534, doi:10.1029/2003JD003470.
- Ginoux, P., M. Chin, I. Tegen, J. M. Prospero, B. Holben, O. Dubovik, and S.-J. Lin (2001), Sources and distributions of dust aerosols simulated with the GOCART model, *J. Geophys. Res.*, 106, 20,255–20,274.
- Hastenrath, S. (1991), *Climate Dynamics of the Tropics*, Kluwer Acad., Dordrecht, Netherlands.
- Herman, J., P. Bhartia, O. Torres, C. Hsu, C. Seftor, and E. Celarier (1997), Global distribution of UV-absorbing aerosols from Nimbus 7/TOMS data, *J. Geophys. Res.*, 102, 16,911–16,922.
- Hsu, N. C., S.-C. Tsay, M. King, and J. R. Herman (2004), Aerosol properties over bright-reflecting source regions, *IEEE Trans. Geosci. Remote Sens.*, 42, 557–569.
- Hsu, N. C., S.-C. Tsay, M. King, and J. R. Herman (2006), Deep Blue retrievals of Asian aerosol properties during ACE-Asia, *IEEE Trans. Geosci. Remote Sens.*, 44, 3180–3195.
- Klein Goldewijk, K. (2001), Estimating global land use change over the past 300 years: The HYDE database, *Global Biogeochem. Cycles*, 15, 417–433.
- Koren, I., and Y. J. Kaufman (2004), Direct wind measurements of Saharan dust events from Terra and Aqua satellites, *Geophys. Res. Lett.*, 31, L06122, doi:10.1029/2003GL019338.
- Legrand, M., A. Plana-Fattori, and C. N'doumé (2001), Satellite detection of dust using the IR imagery of Meteosat: 1. Infrared difference dust index, *J. Geophys. Res.*, 106, 18,251–18,274.
- Maring, H., D. L. Savoie, M. A. Izaguirre, L. Crustals, and J. S. Reid (2003), Mineral dust aerosol size distribution change during atmospheric transport, *J. Geophys. Res.*, 108(D19), 8592, doi:10.1029/2002JD002536.
- Mahowald, N. M., and C. Luo (2003), A less dusty future?, *Geophys. Res. Lett.*, 30(17), 1903, doi:10.1029/2003GL017880.
- Mahowald, N. M., J. A. Ballantine, J. Feddema, and N. Ramankutty (2007), Global trends in visibility: Implications for dust sources, *Atmos. Chem. Phys.*, 7, 3309–3399.
- Martin, J. H., R. M. Gordon, and S. E. Fitzwater (1991), The case for iron, *Limnol. Oceanogr.*, 36(8), 1793–1802.
- Mortimore, M., and W. Adams (1999), *Working the Sahel: Environment and Society in Northern Nigeria*, Routledge, London.
- Moulin, C., and I. Chiapello (2006), Impact of human-induced desertification on the intensification of Sahel dust emission and export over the last decades, *Geophys. Res. Lett.*, 33, L18808, doi:10.1029/2006GL025923.
- Neff, J. C., A. P. Ballantyne, G. L. Farmer, N. M. Mahowald, J. L. Conroy, C. C. Landry, J. T. Overpeck, T. H. Painter, C. R. Lawrence, and R. L. Reynolds (2008), Increasing eolian dust deposition in the Western United States linked to human activity, *Nat. Geosci.*, 1, 189–195, doi:10.1038/ngeo133.
- Osborne, S. R., B. T. Johnson, J. M. Haywood, A. J. Baran, M. A. J. Harrison, and C. L. McConnell (2008), Physical and optical properties of mineral dust aerosol during the dust and biomass-burning experiment, *J. Geophys. Res.*, 111, D00C03, doi:10.1029/2007JD009551.
- Prospero, J. M., P. Ginoux, O. Torres, S. E. Nicholson, and T. E. Gill (2002), Environmental characterization of global sources of atmospheric soil dust identified with the Nimbus 7 Total Ozone Mapping Spectrometer (TOMS) absorbing aerosol product, *Rev. Geophys.*, 40(1), 1002, doi:10.1029/2000RG000095.
- Schepanski, K., I. Tegen, B. Laurent, B. Heinold, and A. Macke (2007), A new Saharan dust source activation frequency map derived from MSG-SEVIRI IR-channels, *Geophys. Res. Lett.*, 34, L18803, doi:10.1029/2007GL030168.
- Schepanski, K., I. Tegen, M. C. Todd, B. Heinold, G. Bönnisch, B. Laurent, and A. Macke (2009), Meteorological processes forcing Saharan dust emission inferred from MSG-SEVIRI observations of sub-daily dust source activation and numerical models, *J. Geophys. Res.*, 114, D10201, doi:10.1029/2008JD010325.
- Swap, R., M. Garstang, S. Greco, R. Talbot, and P. Kallberg (1992), Saharan dust in Amazon Basin, *Tellus Ser. B*, 44, 133–149.
- Tegen, I., S. P. Harrison, K. Kohfeld, I. C. Prentice, M. Coe, and M. Heimann (2002), Impact of vegetation and preferential source areas on global dust aerosol: Results from a model study, *J. Geophys. Res.*, 107(D21), 4576, doi:10.1029/2001JD000963.
- Todd, M. C., R. Washington, J. V. Martins, O. Dubovik, G. Lizcano, S. M'Bainayel, and S. Engelstaedter (2007), Mineral dust emission from the Bodélé Depression, northern Chad, during BoDEX 2005, *J. Geophys. Res.*, 112, D06207, doi:10.1029/2006JD007170.
- Washington, R., M. C. Todd, S. Engelstaedter, S. M'bainayel, and F. Mitchell (2006), Dust and the low-level circulation over the Bodélé Depression, Chad: Observations from BoDEX 2005, *J. Geophys. Res.*, 111, D03201, doi:10.1029/2005JD006502.
- Yoshioka, M., N. Mahowald, J.-L. Dufresne, and C. Luo (2005), Simulation of absorbing aerosol indices for African dust, *J. Geophys. Res.*, 110, D18S17, doi:10.1029/2004JD005276.
- Zender, C. S., D. Newman, and O. Torres (2003), Spatial heterogeneity in aeolian erodibility: Uniform, topographic, geomorphologic, and hydrologic hypotheses, *J. Geophys. Res.*, 108(D17), 4543, doi:10.1029/2002JD003039.
- Zender, C. S., R. L. Miller, and I. Tegen (2004), Quantifying mineral dust mass budgets: Terminology, constraints, and current estimates, *Eos Trans. AGU*, 85, 509–512.

D. Garbuзов, Department of Computer Sciences, Princeton University, NJ 08542, USA. (dmitri@princeton.edu)

P. Ginoux, Geophysical Fluid Dynamics Laboratory, NOAA, Princeton, NJ 08542, USA. (paul.ginoux@noaa.gov)

N. C. Hsu, NASA Goddard Space Flight Center, Greenbelt, MD 20771, USA. (christina.hsu@nasa.gov)